View metadata, citation and similar papers at core.ac.uk
brought to you by CORE
provided by Scholarly Materials And Research @ Georgia Tech

Performance Assessment of a Distributed Electric Propulsion System for a Medium Altitude Long Endurance Unmanned Aerial Vehicle

Alexander A. Markov*, Gokcin Cinar†, Jonathan C. Gladin‡, Elena Garcia§, Russell K. Denney¶ and Dimitri N. Mavris‖
Aerospace Systems Design Laboratory, School of Aerospace Engineering,
Georgia Institute of Technology, Atlanta, Georgia 30332

Soumya S. Patnaik**
Aerospace Systems Directorate, Air Force Research Laboratory, Dayton, Ohio 45433

Distributed propulsion systems are enabled by electrified aircraft and can provide aero-propulsive benefits. The magnitude and impact of these benefits rely on the location of propulsors on the vehicle, the amount of propulsive force generated by those propulsors, vehicle geometry, and the extent of hybridization of the propulsion system. With an increased number of degrees of freedom over conventionally electrified aircraft, the full extent of the impacts of this technology have not yet been explored, especially for military applications. This study builds on a previous one that implemented a series hybrid and turboeletric propulsion architecture on a turboprop UAV, by introducing a distributed electric propulsion system on the same vehicle. The previous study showed that with a hybrid architecture, the same performance, in terms of range and endurance, could not be achieved for a fixed gross take-off weight. This study investigates the impact of the distributed propulsion system with the goal of identifying the benefits over the previous vehicle and determining the level of technology required to break even with the conventional propulsion UAV. In incorporating the new propulsion system, the engine and main motor are resized, leading edge wing mounted propellers and motors are added to the configuration, and a new battery sizing strategy is implemented. Preliminary results show that, although this new system shows increased range and endurance over the series hybrid vehicle, it still falls short compared to the conventional vehicle with current levels of technology. Although improvements are needed to the electrical system technology to reduce the weight enough to break even with the conventional system, the new vehicle shows increased performance during climb, and has the capability to store energy during the mission. With the proper power management and battery utilization strategies, this system can provide reduction in fuel burn and improved performance during certain phases of the mission which could be beneficial for military applications.

I. Introduction

DISTRIBUTED Electric Propulsion (DEP) is a method of implementing electrified aircraft propulsion (EAP) that employs multiple motors and propulsive devices to produce lift or thrust for an aircraft. This technology can reduce fuel burn, noise, and emissions and provide an aerodynamic benefit to offset some of the weight penalty often seen with electrified aircraft. This technology has already been implemented by NASA on their X-57 as well as many vehicles intended for advanced air mobility [1]. While the benefits of its application on commercial vehicles have been more thoroughly explored, its application to Unmanned Aerial Vehicles (UAVs) has received less attention.

This paper will investigate the potential benefits of applying DEP to a UAV by building on the foundation developed for the electrification of a medium-altitude long endurance UAV [2]. The goal of the previous study was to develop a

*Graduate Research Assistant, ASDL, School of Aerospace Engineering, Georgia Tech, AIAA Student Member
†Research Engineer II, ASDL, School of Aerospace Engineering, Georgia Tech, AIAA Member
‡Research Engineer II, ASDL, School of Aerospace Engineering, Georgia Tech, AIAA Member
§Senior Research Engineer, ASDL, School of Aerospace Engineering, Georgia Tech, AIAA Member
¶Research Engineer II, ASDL, School of Aerospace Engineering, Georgia Tech, AIAA Member
‖S.P. Langley Distinguished Regents Professor and Director of ASDL, School of Aerospace Engineering, Georgia Tech, AIAA Fellow
**Principal Engineer, Aerospace Systems Directorate, Air Force Research Laboratory, AIAA Senior Member

hybrid and turboelectric propulsion architecture for a conventional UAV and compare the performance under different battery utilization strategies. For a more fair comparison of hybrid architectures, the gross takeoff weight of the vehicle and geometry were kept constant and any additional weight due to the addition of electrical components was deducted from the fuel weight. This study will be summarized to provide background on the work done so far and to lay the groundwork for this continuation study.

A literature review of turboprop UAVs was performed using public domain data and used to determine an appropriate baseline vehicle. The baseline chosen was modeled after a medium altitude long endurance (MALE) UAV for its size, performance, intended mission, and availability of data. Next, a series propulsion architecture, pictured in Figure 1 below, was developed in an in-house tool called Electrified Propulsion Architecture Sizing and Synthesis (EPASS), such that the battery could be disconnected resulting in a turboelectric architecture. More information on the sizing and synthesis tool is available in Ref. [3, 4] The series architecture allows for a source of power to be carried on the vehicle which does not lapse with altitude like an internal combustion engine and can be recharged and used again during the mission. The turboelectric variant does not provide an additional source of power but allows the turboprop engine to be decoupled from the propeller and thus allows both the engine and propeller to be operated more efficiently.

The TPE331-10 turboprop engine was chosen for the vehicle because it matched the required power and size of similar sized UAVs and was modeled using published data from Honeywell which provided maximum operating power and fuel flow for different flight speeds and altitude along with engine weight [5]. Some components were deemed redundant with the addition of a battery and decoupling of the engine and propeller which provided a small weight savings. The Hamilton Standard maps for four-bladed propellers were used to model the propeller performance, and the map used was chosen such that it maximized the efficiency of the propeller during cruise flight conditions.

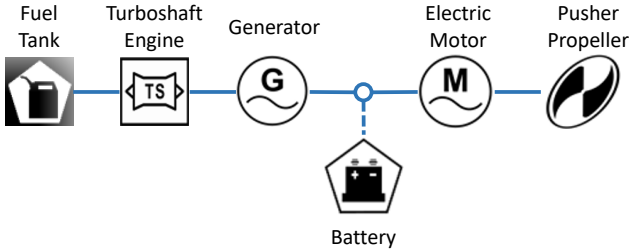

Fig. 1 Schematic of a hybrid turboelectric powertrain.

Along with the engine and propeller, electrical components were modeled to implement the series architecture. This included a generator to convert shaft power from the engine to electric power, and an electric motor to drive the propeller. The generator was sized to the maximum power requirement of the engine during takeoff, as was the motor. Performance maps for these electrical components were also created to model their off-design performance and the technology was based on state-of-the-art generators and motors by Honeywell and Siemens.

A simple battery model was also used which allowed different levels of hybridization to be tested. In this context, hybridization refers to the ratio of battery power to the total power on the vehicle. A battery charging and discharging logic was implemented so that different battery usage strategies could be tested, and it was shown that with the addition of a battery, the vehicle could climb to its cruising altitude faster and store energy and power throughout the mission. However, with the gross takeoff weight being fixed, and the addition of electrical system weight, this meant that the vehicles endurance was reduced as fuel weight was traded for electrical system weight.

To build on the previous research and explore the feasibility space of hybrid UAVs, distributed electric propulsion will be implemented on the same vehicle. Distributed electric propulsion was chosen because it utilizes the electric power on board the vehicle more efficiently and does not required a drastic change in configuration. Additionally, the technology can be applied to both a series architecture as well as a turboeletric architecture which provides a more meaningful comparison to the previous vehicle. As with the previous study, the maximum take-off weight of the vehicle will be kept constant throughout the performance analysis. A more detailed description of the application of the DEP model and its impacts will be discussed in the following section followed by additional changes to the vehicle and case studies to compare the performance of the distributed electric propulsion vehicle to the hybrid electric and baseline vehicles.

II. Distributed Electric Propulsion Modeling

A. Distributed Propulsion Model

Distributed electric propulsion is the synergy of two key technologies: electric propulsion, and distributed propulsion. In previous work, a hybrid electric propulsion system was designed and tested, and some of the benefits of a series hybrid architecture were identified [2]. In order to enable the use of the DEP system, a distributed propulsion system must be introduced and incorporated into the previous propulsion architecture. While a variety of locations and distributions are possible, a leading edge distributed propulsion configuration was chosen because its physics are better understood than more exotic configurations, it is more practical to apply to an existing vehicle, and it can provide an aero-propulsive benefit for the intended mission.

The leading-edge configuration consists of propulsors, in this case propellers, on the leading edge of the wings to provide thrust, and to produce additional lift through improved aero-propulsive efficiency. This occurs because the propellers create an induced velocity that is greater than the freestream, which results in an improved lift-to-drag ratio. This same technology has been used to study NASAs X-57 aircraft utilizing the blown wing effect during take off to reduce required take-off power.

The model used to capture the impacts of this technology is adapted from a study performed by Delft University, which proposed a preliminary sizing method for tube and wing vehicles utilizing leading edge distributed electric propulsion [6]. The study develops a model to estimate the delta lift and drag coefficients of the wings due to an arbitrary number of wing mounted propulsors. The delta aerodynamic coefficients are dependent on wing geometric parameters, the percentage of thrust provided by the distributed propulsors, the size and number of propulsors, as well as parameters like incidence angles and propulsor axial location relative to the leading edge. Figure 2 below shows some of the main parameters used in the model over the half span of an aircraft. Here, b is the span of the aircraft, D_p is the diameter of the propulsor, $\tilde{b}_{dp}$ is the portion of the span affected by the distributed propulsion, δ_y is the spanwise propulsor separation parameter, and N is the total number of propulsors on the wings.

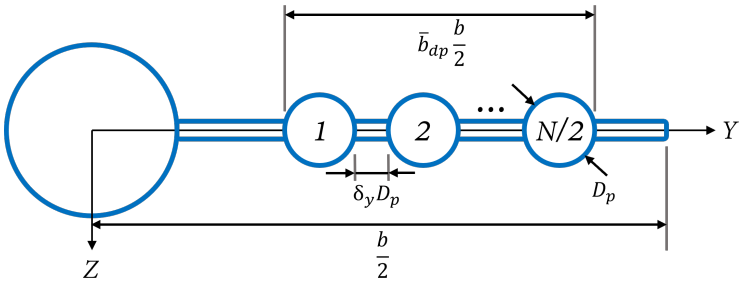

Fig. 2 Example of the distributed propulsion model with main geometric parameters adapted from [6].

In order to avoid overestimating the aero-propulsive benefit of the distributed propulsion, a finite slipstream correction factor, β, is used. This factor acts as a scaling parameter on the induced slipstream velocity to account for the finite slipstream height of the propellers, and to estimate a more accurate and conservative benefit. This correction factor was introduced by Patterson in assessing the benefits of blown wing configurations, and a surrogate model was used to estimate β as a function of the propeller radius to wing chord ration, induced velocity ratio, and the ratio of the axial location from the leading edge to the wing chord [7]. The surrogate model developed by Patterson was verified with computation fluid dynamics (CFD) and ranges for the inputs to the model were stated. More information on the specific parameters used to calculate the delta aerodynamic coefficients, as well as the surrogate model used to calculate β, can be found in the study by Delft University and Patterson's thesis respectively [6, 7].

Although the model is generalizable to more novel configurations and is capable of handling sizing changes to the vehicle, the aircraft weight and geometry in this study, as with the previous study, are held constant. This is done to allow for a fair comparison as vehicle redesign is not in the scope of this research. As such, the wing geometry is the same as the baseline vehicle from the previous study, with the difference in configuration being the addition of leading-edge mounted propellers. This assumption means that some of the input parameters to the distributed propulsion model are fixed, and that there are additional constraints caused by the vehicle geometry. Some similar UAVs have the capability to carry external payload and weapons that are stored on the wing and mounting propellers across the span of the wing may interfere with some of these stores, so the number of propulsors is limited to two for each wing (4 total). There is also a

constraint of 1.2 meters on the maximum diameter of the wing mounted propellers because of ground clearance [8].

With the constraints imposed by the vehicles geometry, and the allowable ranges cited by Patterson for the surrogate models of the finite slipstream parameter, the largest contributor to the aerodynamic benefit of the blown wing is the thrust split parameter, λ_{ts}. This parameter defines the ratio of thrust provided by the wing mounted propellers to the total thrust produced by the vehicle and an example is provided in Figure 3. In this example, 80% of the total thrust is provided by the pusher propeller, and 20% is provided by the wing mounted propellers, where each propeller provides 5% of the total thrust.

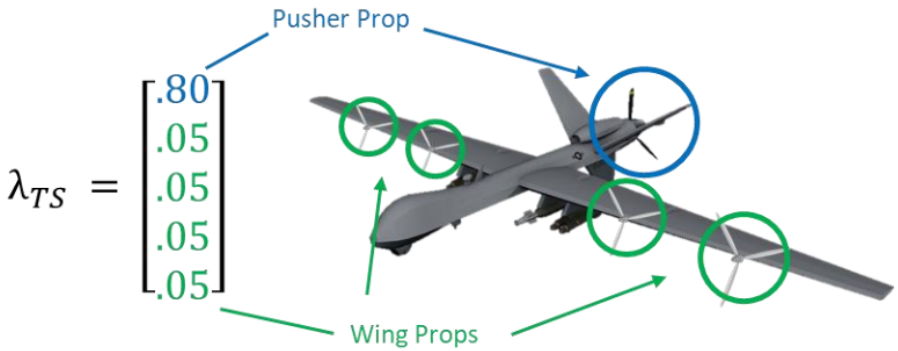

Fig. 3 Notional example of the thrust split parameter.

As mentioned, the imposed constraints limit the degrees of freedom in the distributed propulsion model as applied to the hybrid MALE UAV and the greatest contributor to the aerodynamic benefit is the thrust split parameter. However, the constraints also limit the maximum thrust split because of the allowed ranges of the surrogate model, and this means that the aerodynamic benefit is also bounded by these constraints. The maximum thrust split for these constraints and assumptions is approximately 15%, which results in an increase in the lift-to-drag ratio of the vehicle by 20%. Without more detailed knowledge of the geometry of the vehicle or higher fidelity models like CFD, this is the maximum expected benefit of the distributed propulsion, and this is what will be used to determine the performance benefits of the new configuration.

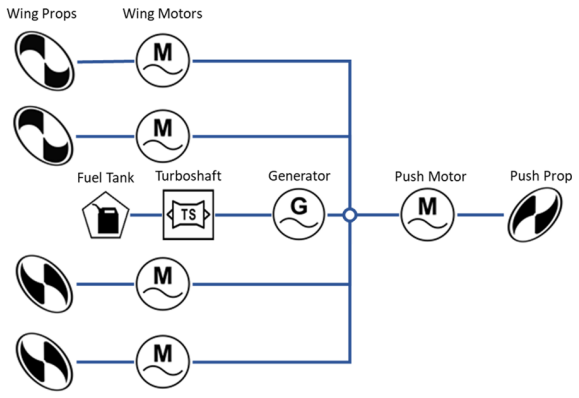

(a) Turboelectric distributed electric propulsion architecture.

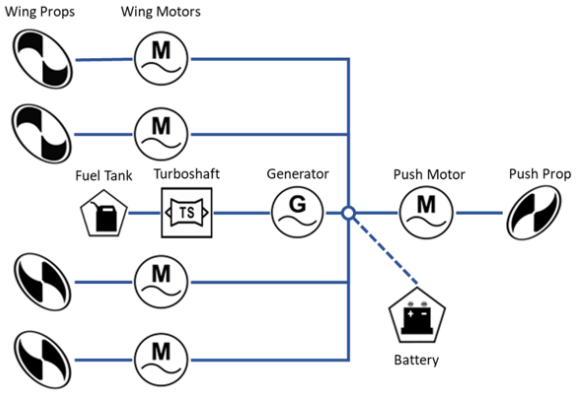

(b) Series distributed electric propulsion architecture.

Fig. 4 Updated propulsion architectures.

With the implementation of this distributed propulsion model, the propulsion architectures were updated to reflect these changes. Figure 4 shows the architecture and powertrain layout for the Turboelectric vehicle in Figure 4a, and for the Series hybrid vehicle in Figure 4b. In the turboelectric vehicle, the generator powers both the wing motors and the pusher motor. The Series vehicle is similar but has a battery attached to supplement power to the pusher motor and wing motors with the capability of recharge from the generator.

B. Motors and Propellers

Before the wing mounted propellers and motor are sized, it is important to consider the other parts of the propulsion system that are affected by these new additions. Now that 15% of the thrust is being offloaded to the wing mounted propellers, the motor for the main pusher propeller can be downsized accordingly. This allows for some weight savings and provides a better comparison between the series hybrid propulsion vehicle and the distributed electric propulsion vehicle. Additionally, the performance map used for the pusher propeller was reexamined when determining which map to use for the wing mounted propellers. A new map was chosen which provided an increase in efficiency during cruise conditions and both the series vehicle propeller and distributed propulsion vehicle propeller were updated and run with this new map.

The resized motor parameters were modeled after a 260 kW electric motor developed by Siemens for use on aircraft. The motor model is based on a loss-based electric motor model that builds up efficiency maps based on frictional, windage, iron, copper, and parasitic losses in an electric motor [9]. The specific power remains 5.22 kW/kg and the maximum efficiency is 95%, however the maximum output power has been decreased from 750 kW to 638 kW in the DEP vehicle, resulting in a weight savings of 47 lbs. It should be noted that the specific power of the motors and generator include the weight of the inverter and rectifier bridge. A new motor performance map was created with this update and is pictured in Figure 5 below. The RPM of the motors are being kept constant throughout the mission which can be represented as a vertical line on this map so performance changes will be a result of changes in the required torque, and thus changes in required thrust and power. This is represented in Figure 5 with the operating points for the take-off (TKO), climb, and cruise segments. Similar motor performance maps were created for the motors powering the wing mounted propellers. These motors have the same specific power and efficiency but have a maximum output power of 28 kW each. Because of the difference in required power and flight conditions throughout the mission, a variable speed motor is something that could potentially provide a benefit to motor performance and efficiency but is out of scope for this study.

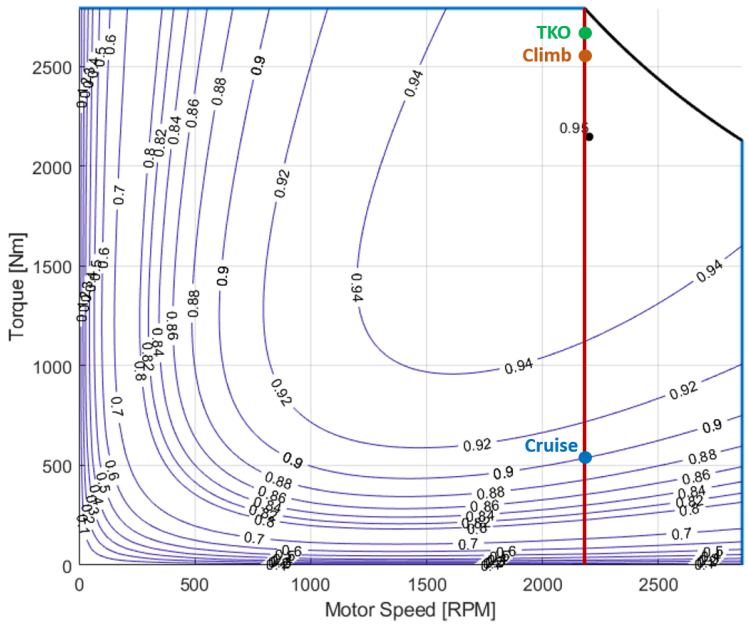

Fig. 5 Motor performance map for the pusher motor on the distributed electric propulsion vehicle.

The next step of implementing the wing mounted propellers is determining which propeller map to use in order to maximize their performance. Four bladed Hamilton Standard propeller maps were considered with varying design lift coefficients and activity factors. For the wing mounted propellers, a map with a design lift coefficient of 0.3 and activity factor of 80 was chosen to both maximize the efficiency for cruise flight conditions and to reduce the weight of the propellers. Although the advance ratio is known, a simple visual check of the propeller map is not enough to determine maximum efficiency because the map cannot determine if the propeller can provide the required thrust during cruise. An example of this is shown in Figure 6 below which shows a notional propeller performance map with different design points, indicated by different RPM data labels, superimposed.

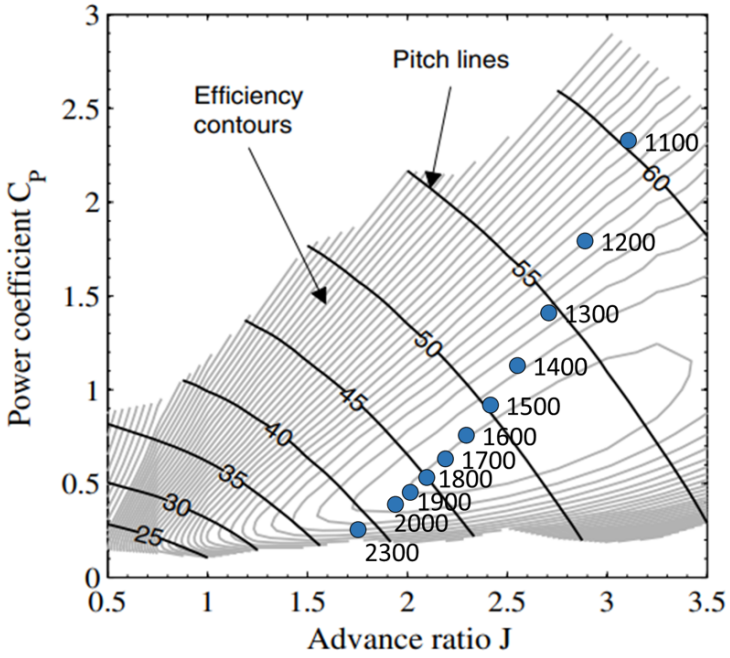

Fig. 6 Notional propeller performance map with design points superimposed (adapted from [10]).

These design points assume that the pitch angle of the propellers is a fallout such that the efficiency is maximized, however, the map by itself cannot check whether or not the propeller can provide the required thrust. This is addressed by performing both a torque and thrust check in E-PASS, the sizing and synthesis environment, by calculating the torque and thrust coefficients and choosing a pitch angle that ensures torque and thrust are realizable. By doing so, the design point for a given RPM on the map shifts to the pitch angle determined by E-PASS, resulting in a change in efficiency. The maps themselves cannot be used to determine the design point of the propellers so several maps were tested before the chosen map was identified.

Finally, with the propeller performance map chosen, the propeller weight can be calculated by looking at weight regression equations provided by the Hamilton Standard documentation. Two regressions are available, one for traditional blades and one for fiberglass blades which offer a lighter weight propeller. This fiberglass regression, shown in Equation 1, was chosen because current state-of-the-art technology is assumed, and a lighter weight propeller is expected.

$$W_{prop} = \left[\left(\frac{D}{10} \right)^{1.85} \left(\frac{B}{4} \right)^{0.7} \left(\frac{AF}{100} \right)^{0.6} \left(\frac{ND}{20000} \right)^{0.5} (M+1)^{0.5} \left(\frac{SHP/D^2}{10} \right)^{0.12} \right] \tag{1}$$

Here, D is the diameter of the propeller in feet, B is the span of the blade in feet, AF is the activity factor, N is the RPM, M is the operational Mach number, and SHP is the shaft horsepower at sea level. In addition to the changes to the propellers and motors in the propulsion system, the engine must be resized because the engine and propeller are decoupled. This allows the performance of both of these components to be improved and potentially allows the engine to be resized depending on the presence and usage of a battery.

III. Engine Remodeling

The series configuration inherently decouples the engine and the propeller allowing both of them to be operated more efficiently. With the addition of a battery, a new degree of freedom is also introduced, the degree of hybridization, which determines how much of the required power is provided by the battery and how much is provided by the engine through the generator. By changing this degree of hybridization, the engine size is allowed to scale as some of the power previously required by the engine can be supplemented by the battery.

In order to be able to resize the engine, an engine model must be created, and appropriate sizing effects must be accounted for to have a realistic model as the engine is scaled. A free power turbine engine architecture was chosen

because it allows the required power to be pulled from the engine by a turbine that is not connected to the main shaft, allowing the engine to operate more efficiently while still providing the necessary amount of power. Historical regressions of similar engines were used to determine the engine performance and weight for two sizing conditions: Take-off power and cruise power. The model of the engine sized for take-off power is used to generate engine decks for the baseline vehicle and the turboelectric vehicle, while the model of the engine sized for cruise power is used to generate an engine deck for the series distributed propulsion vehicle. This ensures that comparisons to the baseline vehicle remain consistent.

The engine models and engine decks are developed in the Numerical Propulsion System Simulation (NPSS) engine cycle analysis environment by iterating the static sea level power, or engine flat rating depending on the method of sizing, to meet power requirements. The power requirements set the cycle pressure ratio and turbine inlet temperature so that the component efficiencies, cooling flows, and total airflow can be determined. The engine weight is then computed based on a historical regression using the engine airflow and power. The results of engine sizing are an estimate of the engine weight and a generated engine deck, both of which are output back to E-PASS for use in the vehicle performance analysis. Figure 7 shows a comparison of the specific fuel consumption between the digitized engine deck and the engine deck output from the NPSS model. The NPSS engine deck shows a lower overall specific fuel consumption and is sized more appropriately for the mission and flight conditions flown.

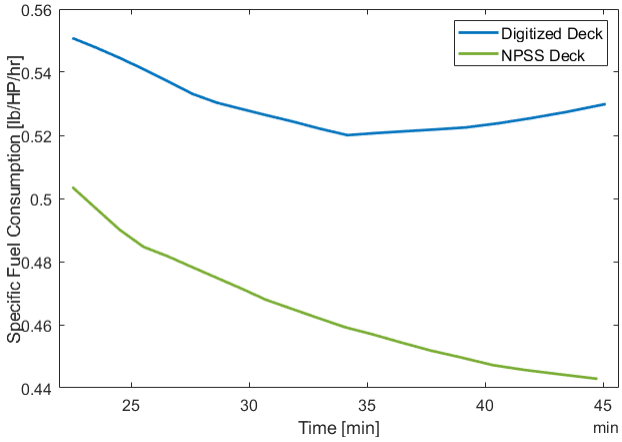

Fig. 7 Specific fuel consumption comparison between the digitized engine deck and the NPSS engine deck.

The engine models also allow for the toggling of a technology switch that implements component efficiency improvements and weight reduction estimated for 2030 projections. This enables a study to be performed on the impacts of engine technology that are isolated from the electrical components. The impacts include a reduction in specific fuel consumption, as seen in Figure 8, due to improved efficiency, as well as some fuel weight. The assumptions behind these impacts are based on NASA's revolutionary vertical lift technology study and result in a BSFC improvement of ~15% and an engine horsepower to weight ratio improvement of ~16% [11]. The maximum take-off weight of the vehicle is held constant so weight savings from a lighter engine translate to some additional fuel weight up to the maximum fuel capacity of the vehicle. For example, an engine sized for cruise power using current state of the art technology weighs about 278 pounds, while an engine sized for the same power requirement under 2030 technology assumptions weighs 261 pounds. This weight reduction and trade-off is true for both the engine sized for take-off power and the engine sized for cruise power, although the downsized engine requires battery assist, so battery weight must be accounted for.

The downsized engine for the series configuration allows for a power shaving technique to be implemented so that the engine is operating closer to its optimal efficiency throughout take-off, climb, and cruise. This is because an engine sized for take-off will be larger and thus will need to be throttled down during cruise causing the efficiency to drop. However, by power shaving the engine, additional power is needed during take-off to meet the power requirements so a battery must be used to assist. For this study, the series configuration utilizes a battery to supplement power during take-off as well as during the climb segment to provide a boost to climb performance. The engine is slightly oversized so that it can provide the additional power required to charge the battery during cruise.

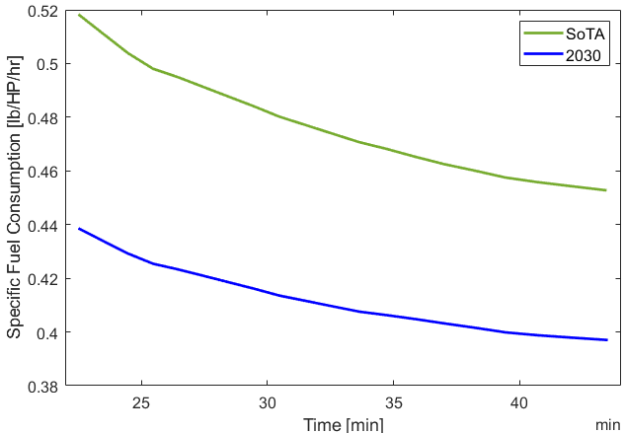

Fig. 8 Specific fuel consumption comparison between the current technology and 2030 projected technology.

IV. Improved Powersplit Strategy

A new strategy for determining the powersplit between the generator and the battery was developed and implemented on the series vehicle. Where the previous powersplit was an input, using the new strategy, it is a fallout. Rather than setting a powersplit value using some prior knowledge or assumptions, the power for pusher motor is held constant, and the generator and battery power split values are a fallout. As the engine lapses with altitude, the generator power decreases, causing the generator powersplit to decrease, and the battery provides more power causing the battery powersplit to increase. In this way, the powersplit no longer has to remain constant, and a more practical application of hybridization is implemented. An example of this is shown in Figure 9. This allows the vehicle to operate with a higher specific power at altitude to improve climbing performance and reduce time to climb. This battery power management approach is called and electric power boost strategy.

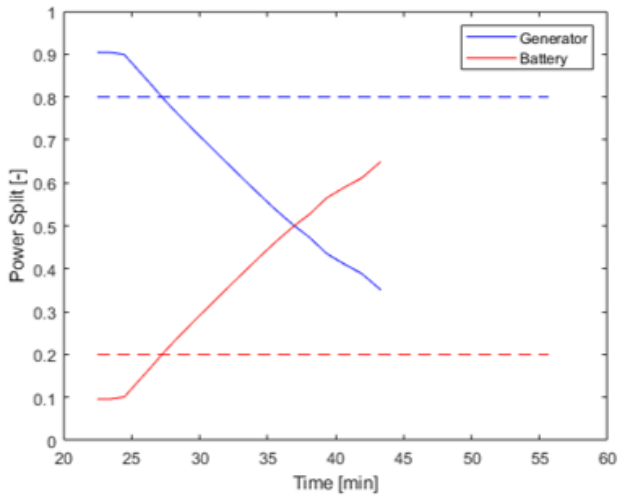

Fig. 9 Example powersplit values during the climb segment for the series vehicle.

The dashed lines represent the previous method of setting the powersplit values and having them remain constant throughout the duration of the segment while the solid lines represent the new strategy. Initially the generator is providing a majority of the power to the pusher motor, but as the vehicle climbs, the generator power lapse and the battery power increases as reflected in the powersplit changes. This same approach can be used during other mission segments, but if the altitude and flight conditions are constant, the powersplit values will remain constant as well.

V. Payload-Range Study

The Baseline, Turboelectric, and Series Hybrid vehicles in this study are not being redesigned and thus their maximum take-off weights remain constant. Therefore, as additional weight is added from electrical components, propellers, and batteries, weight must be traded from either the payload or the fuel weight to maintain a constant total weight. As such, it is expected that the payload of the hybridized vehicles will decrease below the maximum payload value of the baseline vehicle, but it is not clear whether the performance of the vehicle will improve. To determine the impact of the distributed electric propulsion and hybridization on the vehicles, a payload range study is performed. The goal of this study is to determine how much of an impact this technology has on vehicle performance and if it can outweigh the additional weight associated with hybridization. While this particular study focuses on the range, the addition of a battery was shown to benefit the climb performance of the vehicle by providing excess power that does not lapse with altitude. This is a significant benefit that is not reflected in the payload range study but should be considered when analyzing the effectiveness and impact of the hybrid system.

The results of the payload-range study are shown in Figure 10 where the baseline is in blue, the turboelectric is green, and the series hybrid is red. The maximum payload of the baseline vehicle is 3800 pounds while the maximum payloads of the turboelectric and series hybrid are approximately 3200 pounds and 1600 pounds respectively. All three vehicles were run for the same mission with a free cruise segment. This free cruise segment is allowed to vary in terms of endurance so that the amount of fuel required is equal to the amount of fuel available. Fuel required is calculated by running the vehicle through the mission and available fuel is calculated by determining the amount of weight left after subtracting the empty weight, propulsion system weight including electrical components, propeller weight, payload weight, and accounting for any weight saved from reduction in engine size or removal of any unnecessary engine component with the addition of a battery.

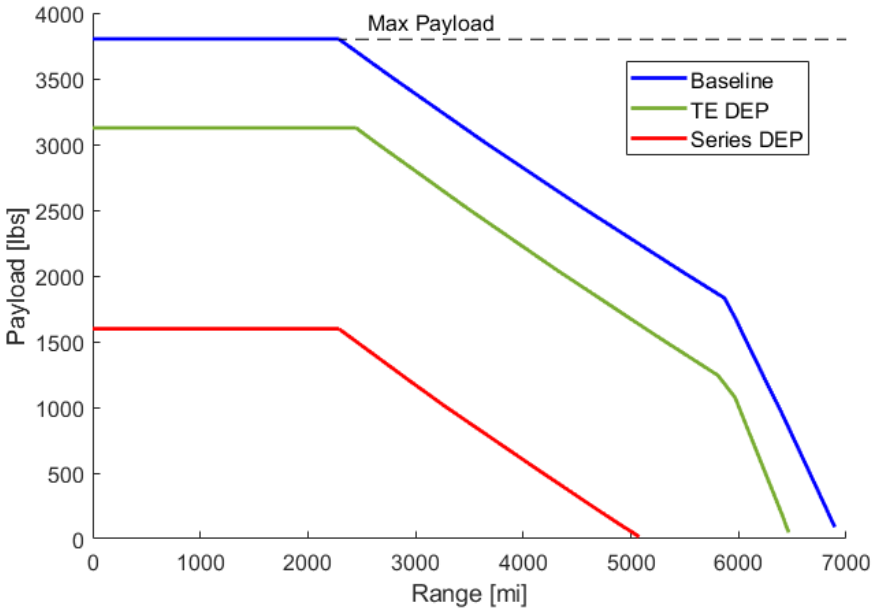

Fig. 10 Payload range diagram for the baseline, turboelectric, and series hybrid vehicles.

As mentioned before, the maximum fuel capacity was also taken into account by capping the amount of weight that can be traded. This is relevant for cases with smaller payload values because it essentially allows more fuel to be added, but the fuel tanks can only hold a certain amount of fuel. For cases where the payload is decreased further and no additional fuel can be added, the maximum take-off weight is decreased. The vehicle is not resized, rather it is flying with maximum fuel capacity but with less than the maximum payload than it can carry with the fuel. This allows the vehicle to fly a bit further with the same amount of fuel because it is carrying less weight overall and is represented by the steeper sections of the plot. The series hybrid vehicle does not show this trend because even with no payload, the weight of the electrical components and battery are enough to detract from the fuel weight such that the maximum capacity is not reached. Given the current state of the art technology assumptions, neither the turboelectric or series hybrid can out perform or even match the range performance of the baseline. Again, climb performance was shown to

improve, but in terms of range, the hybrid vehicles show a decreased performance relative to the baseline.

To better understand the differences between the architectures, the weights of the propulsion systems will be broken down and compared. In addition, the fuel used and the available payload will also be compared as for a fixed MTOW, these two will be traded for any additional propulsion system weight. The maximum payload cases, represented by the horizontal line just before payload begins to decrease, for each will be compared. Table 1 shows the weight build up for all three vehicle architectures, and also compares the total propulsion system weight and range. The fuel weight does not change much across the architectures which is expected given that this comparison is looking at essentially the same range values as indicated at the bottom of the table. However, with the addition of electrical components, the propulsion system weight drastically increases, and payload must be traded. It is clear that given the current state of the art technology in electrical components, the weight of the hybridized propulsion system is too much to be overcome by the additional benefit in aerodynamic efficiency from the distributed propulsion system.

Table 1 Architecture weight breakdown and range comparison

	Baseline	TE	Series
MTOW (lbs)	10500	10500	10500
Empty Weight (lbs)	4900	4900	4900
Fuel (lbs)	1789	1859	1695
Payload (lbs)	3802	3093	1603
Engine (lbs)	316	316	278
Engine Accessories (lbs)	180	80	80
Generator (lbs)	-	416	416
Motors (lbs)	-	269	269
Wing Props (lbs)	-	63	63
Battery (lbs)	-	-	1692
Total Propulsion System (lbs)	496	1144	2798
Range (nmi)	2285	2447	2287

Although current state of the art technology is not enough to enable the hybrid vehicles to out perform the range of the baseline, perhaps better technology can provide more benefit. To investigate this, a technology trade study was performed focusing on the electrical component specific power, specific energy, and efficiency.

VI. Technology Sensitivity Studies

The electrical component technology was projected to 2030, 2040, and 2050 time frames to better understand how the evolution of technology will impact the vehicles. The current state of the art technology assumptions have already been discussed in this and the previous study so they will not be covered again here. The specific power and efficiency of the electric motors and the generator as well as the specific energy of the battery pack were projected by starting with a baseline value from 2016 based on the research of NASA and the National Academies of Sciences, Engineering, and Medicine [12]. For the purposes of the technology projection, the electric motors and generator are treated as the same component. The medium confidence interval values from the study were used to avoid overoptimistic assumptions while also considering that additional changes and improvements would be made to other parts of the vehicle that are not captured in this study. The assumed annual growth of the specific power of the electric motors is 7% and the assumed annual growth of the specific energy of the battery is 3.5%. The values used for the three time frames are shown in Table 2 based on the annual improvements up to the year of the time frame. The efficiency of the electric motors and generator are assumed to increase by 1% each decade up to 98% in 2050. It should be noted that an optimistic assumption of 250 Wh/kg on the battery pack specific energy was assumed for current state of the art.

To investigate the impacts that these assumptions have on vehicle performance, the turboelectric vehicle will be compared to the baseline. The payload-range diagram for the turboelectric vehicle is shown in Figure 11 with the baseline and current state of the art turboelectric vehicles for reference. Because the turboelectric vehicle does not have a battery, these results only reflect the impacts of the electric motor and generator technology improvements. With the

Table 2 Electric Component Technology Projections

Parameter	2030	2040	2050
Electric Motor Specific Power [kW/kg]	10	20	30
Electric Motor Efficiency [-]	96%	97%	98%
Battery Pack Specific Energy [Wh/kg]	270	325	455

increase in specific power and efficiency, the vehicle has a much higher maximum payload compared to the current state of the art and is quite close to that of the baseline vehicle. The maximum payload will not be quite the same as the baseline because some components are being added and only about 100 pounds are being removed from things like the engine. For the 2040 and 2050 time frames, the vehicle shows an increase in range for essentially all payload values over the baseline. For the 2030 time frame, the vehicle has a maximum payload that is about 500 pounds smaller and is slightly behind in terms of range, expect for small values of payload beyond the maximum fuel capacity limit. This shows promise for hybrid vehicles even without the use of a battery.

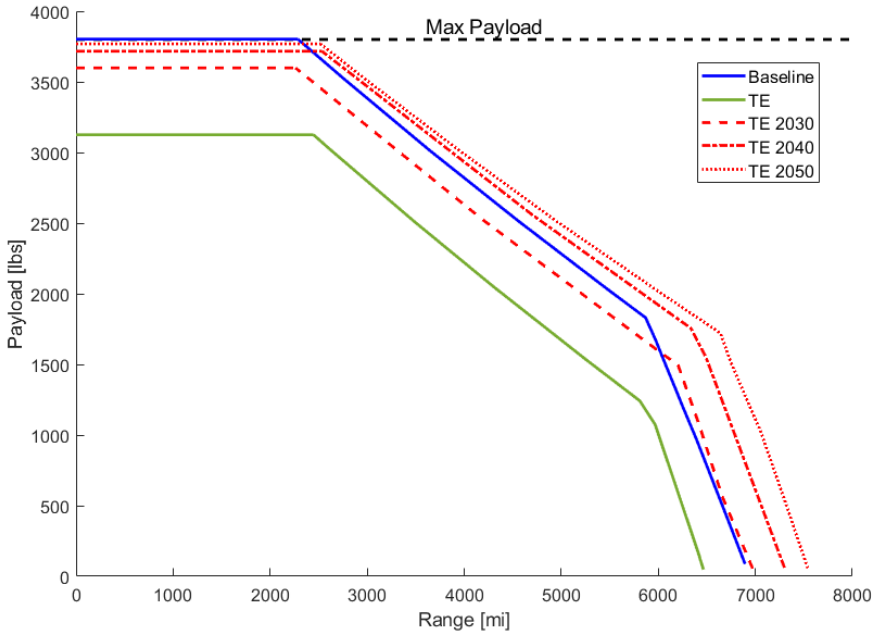

Fig. 11 Payload range diagram comparing the turboelectric for different technology projections.

A similar study was performed for the series hybrid vehicle and is shown below in Figure 12 where the baseline and state of the art series hybrid vehicles are shown. This comparison includes the technology improvements of the electric motors and generator as well as the battery, so the impacts are even more noticeable. While the battery weights are still relatively larger, the reduction in battery weight is significant. In the 2030 time frame the series vehicle still cannot match the baseline performance, but by the 2040 time frame the vehicle is close in terms of range. The obvious decrease in maximum payload is apparent, however, and still results in almost half of the payload being removed to accommodate the electrical components in the 2050 time frame. Here the vehicle shows some improvement but similar to the turboelectric it is for smaller payload values beyond the maximum fuel capacity limit.

The results are also shown below in Figure 13 and are separated by time frame. The baseline, state of the art turboelectric, and state of the art series hybrid are shown in each figure. Figure 13a, Figure 13b, and Figure 13c then show the turboelectric and series vehicles with the respective technology levels of those time frames applied.

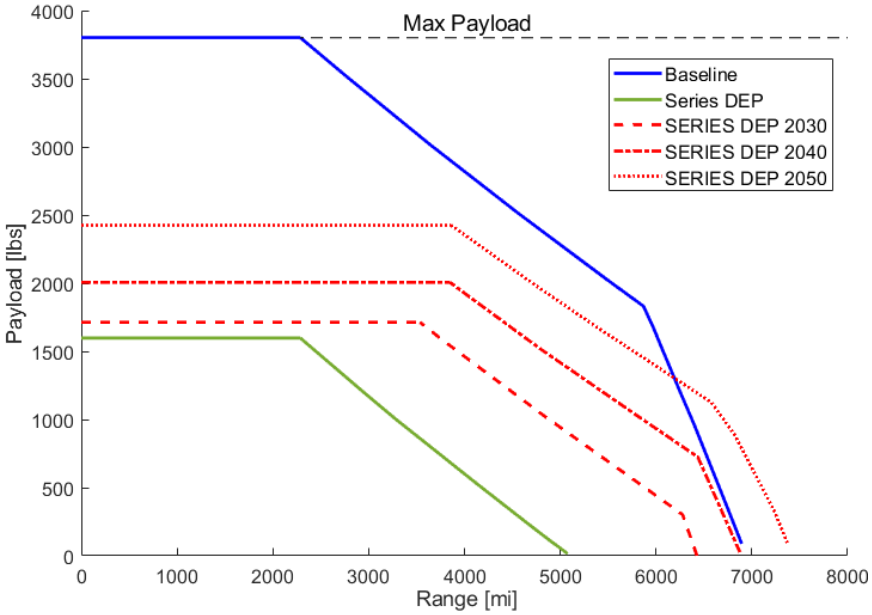

Fig. 12 Payload range diagram comparing the series hybrid for different technology projections.

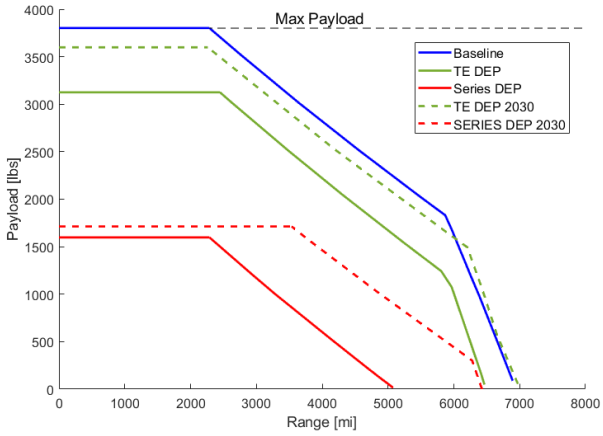

(a) 2030 projections

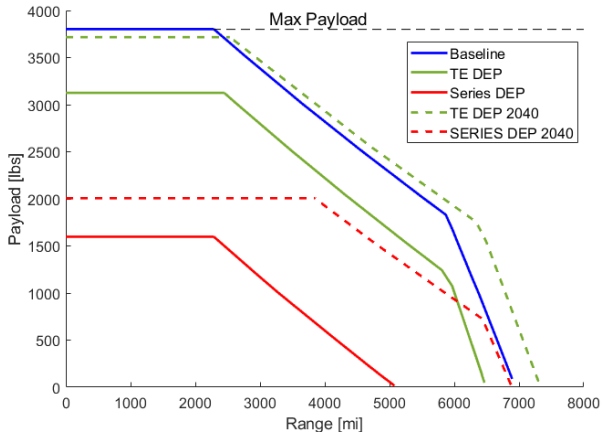

(b) 2040 projections

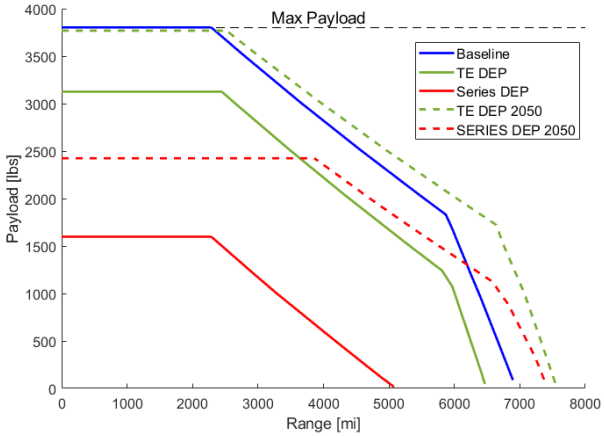

(c) 2050 projections

Fig. 13 Technology impacts based on time frame.

VII. Conclusion and Future Work

A MALE UAV utilizing turboelectric and series hybrid propulsion systems was fitted with four wing mounted propellers to make use of distributed electric propulsion. The utilization of distributed propulsion improves the aerodynamic efficiency of the vehicle and improves performance. The trade-off between the additional weight of the electrical components and the benefit of this system was explored in this paper. It was observed through a payload-range diagram that with current technology the turboelectric and series hybrid vehicles simply did not gain enough benefit to overcome the weight of the addition of the electrical components. Although the climb performance of the vehicles showed some improvement, the range and maximum payload were drastically decreased.

A technology study was also performed to determine how technology projections in the coming decades would impact the vehicle range and maximum payload. This was also explored through the use of a payload-range diagram with technology time frames of 2030, 2040, and 2050. The electric motor specific power and efficiency as well as battery specific energy were projected from state-of-the-art values determined by NASA and annual improvement margins. The results show that by 2040, the turboelectric vehicle near matches the maximum payload and slightly exceeds the baseline vehicles in terms of range, however the series hybrid propulsion system still weighs significantly more than the baseline and therefore has a reduced maximum payload. It also doesn't quite match the baseline in terms of range even by the 2050 time frame.

Based on the current assumptions and the modeling approaches, a turboelectric variant of the baseline vehicle shows an improvement over the baseline by 2040, while a series hybrid variant does not quite breakeven by 2050. The battery used in the series hybrid vehicle is currently sized for cruise power requirements and supplements the engine during take-off and climb, however a different battery utilization strategy could reduce the battery size by reducing the power shaving of the engine. This would increase the engine size and have some impact on the specific fuel consumption, but a trade study was not performed in this study but is of interest for future work. A more optimal propulsion architecture could also provide more benefit by utilizing the battery more efficiently and reducing the number of electrical components and therefore the weight of the propulsion system. This too is of interest but is left for future work. Additional areas of interest are higher fidelity battery models to more accurately capture power requirements, heat loads, and c-rates of the battery and to investigate how they would impact performance and propulsion system implementation. Improving the fidelity of the distributed propulsion system could also provide valuable insight into the optimal number of propellers as well as the optimal size of those propellers. This would also better quantify the impact of this kind of propulsion system for the chosen vehicle configuration.

VIII. Acknowledgments

The authors gratefully acknowledge funding support from AFRL/RQQI under Contract No. S-162-11-MR006. The authors would also like to thank the AFRL Flight Systems Integration Team, including Ryan Miller, Brian Donovan, Adam Donovan, and Nathaniel Smith, for their valuable feedback and support to this work.

References

[1] Borer, N., Derlaga, J., Deere, K., Carter, M., Viken, S., Patterson, M., Litherland, B., and Stoll, A., "Comparison of Aero-Propulsive Performance Predictions for Distributed Propulsion Configurations," Tech. rep., NASA Technical Reports Server, 01 2017.

[2] Cinar, G., Markov, A. A., Gladin, J. C., Garcia, E., Mavris, D. N., and Patnaik, S. S., "Feasibility Assessments of a Hybrid Turboelectric Medium Altitude Long Endurance Unmanned Aerial Vehicle," *AIAA Propulsion and Energy 2020 Forum*, 2020.

[3] Cinar, G., "A methodology for dynamic sizing of electric power generation and distribution architectures," Ph.D. thesis, Georgia Institute of Technology, 2018.

[4] Cinar, G., Garcia, E., and Mavris, D. N., "A framework for electrified propulsion architecture and operation analysis," *Aircraft Engineering and Aerospace Technology*, Vol. 92, No. 5, 2019, pp. 675–684.

[5] Honeywell, "TPE331-10 TURBOPROP ENGINE," Brochure, 2016.

[6] Vries, R., Brown, M., and Vos, R., "A Preliminary Sizing Method for Hybrid-Electric Aircraft Including Aero-Propulsive Interaction Effects," *AIAA AVIATION Forum 2018 Aviation Technology, Integration, and Operations Conference*, 2018.

[7] Patterson, M., "Conceptual Design of High-Lift Propeller Systems for Small Electric Aircraft," Ph.D. thesis, Georgia Institute of Technology, 2016.

[8] DrawingDatabase, "General Atomics MQ-9 Reaper Blueprint," , 2019. URL `https://drawingdatabase.com/mq-9-reaper/`.

[9] Larminie, J., and Lowry, J., *Electric Vehicle Technology Explained*, John Wiley & Sons, 2003.

[10] Giannakakis, P., Goulos, I., Laskaridis, P., Pilidis, P., and Kalfas, A. I., "Novel Propeller Map Scaling Method," *Journal of Propulsion and Power*, Vol. 32, No. 6, 2016, pp. 1325–1332.

[11] Snyder, C., and Tong, M., "Modeling Turboshaft Engines for the Revolutionary Vertical Lift Technology Project," *NASA Technical Reports Server*, 2019.

[12] "Commercial Aircraft Propulsion and Energy Systems Research: Reducing Global Carbon Emissions," *National Academies of Sciences, Engineering, and Medicine*, 2016.